RSC Advances

PAPER

View Article Online
View Journal | View Issue

Cite this: *RSC Adv.*, 2021, **11**, 3342

Solution structure of zinc-seamed *C*-alkylpyrogallol[4]arene dimeric nanocapsules†

Harshita Kumari, *[a] Wei G. Wycoff,[b] Collin M. Mayhan,[b] Steven R. Kline,[c] Joshua R. So,[b] Carol A. Deakyne,*[b] John E. Adams *[b] and Jerry L. Atwood *[b]

Received 27th November 2020
Accepted 29th December 2020

DOI: 10.1039/d0ra10053f

rsc.li/rsc-advances

The structural stability and solution geometry of zinc-seamed-*C*-propylpyrogallol[4]arene dimers has been studied in solution using *in situ* neutron scattering and 2D-DOSY NMR methods. In comparison with the structures of the analogous copper-/nickel-seamed dimeric entities, the spherical geometry of the PgC_3Zn species (R = 9.4 Å; diffusion coefficient = 1.05 × 10^{-10} m^2 s^{-1}) is larger due to the presence of ligands at the periphery in solution. This enhanced radius in solution due to ligation is also consistent with the findings of model molecular dynamics simulations of the zinc-seamed dimers.

A supramolecular assembly can be defined as a complex entity, such as a DNA double helix, held together by non-covalent bonds. Such complex large entities are formed *via* molecular self-assembly, a process taking far fewer steps than does a conventional synthesis of a single molecule of similar dimensions. The ease of formation, high yield, and possible practical applications as functional materials are some of the factors that have spurred a widespread interest in supra- and supermolecular assemblies.[1–6]

One group of such assemblies comprises the metal-seamed pyrogallol[4]arene nanocapsules (Fig. 1).[1,7] Although these nanocapsules have now been synthesized with a selection of alkyl groups, metals, guests and axial ligands, only a few have been examined in solution.[8–15] Our motivation in studying solution-phase architectures is to determine whether the solution structures conform to the solid-state geometries. Many nanocapsules, specifically transition metal (Cu/Ni)-seamed hexamers and dimers and hydrogen-bonded dimers, retain their solid-state geometry in solution.[10,13] In contrast, Ga- and Ga/Zn-seamed pyrogallol[4]arene hexamers rearrange from spheres in the solid state to toroids in solution.[12] Similarly, the hydrogen-bonded PgC_1⊂ferrocene/PgC_6⊂pyrene nanotubes rearrange to dimers in solution.[14,15] Solution-phase studies also have allowed us to discover novel structures of species that were either difficult to crystallize or expected to be unstable in solution.[9,11] For example, the ellipsoidal and tubular architectures of the $PgC_{17}Cu$ and PgC_1Fe nanoassemblies, respectively, have been studied exclusively in solution.[9,11]

The current study and analysis focus on the solution structure of the original dimeric pyrogallol[4]arene-based nanocapsules: [Zn_8(*C*-propylpyrogallol[4]arene)$_2$(pyridine)$_7$(DMSO)$_1$⊂pyridine], with propyl R-groups, a pyridine guest and pyridine/DMSO axial ligands (Fig. 1C and D, propyl R-groups and guest pyridine molecule are removed for clarity).[16] The zinc dimer is composed of two pyrogallol[4]arene subunits that are coordinated by the ring of eight Zn^{+2} ions across the equatorial belt. The metal atoms displace 16 of the 24

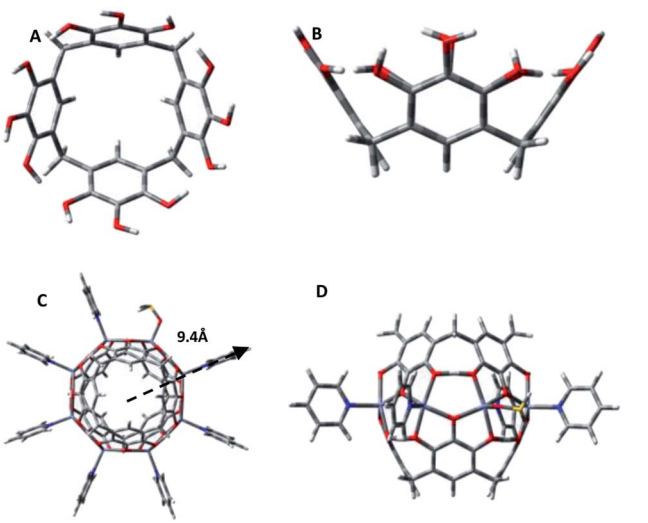

Fig. 1 (A) Top view of pyrogallol[4]arene; (B) front view of pyrogallol[4]arene; (C) top view of the *C*-alkylpyrogallol[4]arene zinc-seamed dimer illustrating the approximate radius of the capsule; (D) front view of the *C*-alkylpyrogallol[4]arene dimer. For clarity alkyl groups and guest pyridine molecule are removed from the figures. O: red, M (metal): light blue, C: grey, N: blue, H: white.

[a]*James L. Winkle College of Pharmacy, University of Cincinnati, OH 45267, USA. E-mail: kumariha@ucmail.uc.edu*

[b]*Department of Chemistry, University of Missouri-Columbia, Columbia, MO 65211, USA. E-mail: AtwoodJ@umsystem.edu; DeakyneC@umsystem.edu; AdamsJE@umsystem.edu*

[c]*NIST Center for Neutron Research, National Institute of Standards and Technology, 100 Bureau Drive, Gaithersburg, MD 20899, USA*

† Electronic supplementary information (ESI) available. See DOI: 10.1039/d0ra10053f

hydroxyl protons of the pyrogallols to seam this spherical framework. Each of the zinc centers is ligated by four phenoxy groups, two from each pyrogallol, along with an axial DMSO or pyridine ligand, that gives a square pyramidal configuration to the metal center. The central phenoxy group from each pyrogallol is bridged between two adjacent zinc centers, whereas the two exterior phenoxy groups are each ligated to a single zinc center and hydrogen-bonded to a phenoxy group on the neighboring pyrogallol subunit, making the overall assembly neutral. In the transition from pentacoordinated Zn in the solid state to tetracoordinated Zn in the gas phase, as a result of the MALDI-TOF analysis, this local Zn–O binding geometry is essentially preserved.[16–18] Of course, thermal fluctuations do occur, although, as we shall show *via* molecular dynamics simulations, the overall shape remains roughly spherical.

The PgC_3Zn dimeric nanocapsule was synthesized by adding 1 equiv. of PgC_3 (0.01 mol L^{-1}), 4 equiv. of zinc(II) nitrate (0.04 mol L^{-1}), and 14 equiv. of pyridine in DMSO solvent. The solution was heated, sonicated, and left overnight to obtain yellow crystals of the dimer. The unit cell was confirmed and the crystals were filtered and dissolved in *d*6-DMSO at mass fractions of 1% and 5% for SANS measurements. Preferential deuteration of solvent for SANS studies enhances the coherent scattering and improves the contrast between the solute and the solvent. The samples were left overnight to ensure saturation without precipitation, and the SANS measurement was conducted at 25 °C on the NG3 30m SANS instrument at the NIST Center for Neutron Research in Gaithersburg, MD.[19] The collected scattering data was reduced and analyzed using IgorPro[20] incorporating the instrumental *q*-resolution function.

The measurements on the dimeric sample at mass fractions of both 1% and 5% were conducted to ensure sufficient scattering and to detect a concentration dependence of the capsular structure. The scattering length densities (SLDs) of the solute and solvent were calculated and held fixed for data analyses. The SLDs of the solvent (*d*6-DMSO) and solute (PgC_3Zn dimer) were fixed at 5.28×10^{-6} Å^{-2} and 1.37×10^{-6} Å^{-2}, respectively.

The reduced SANS data was fitted globally, with the two data sets corresponding to different mass fractions being modelled simultaneously to obtain the best fit. The data was fitted to various cylindrical, ellipsoidal and core–shell models to detect the occurrence of structural transformation. It was quickly found, however, that the entity does not have a core–shell, ellipsoidal or cylindrical geometry (ESI†). Previous studies on copper and nickel nanocapsules have indicated the presence of both dimers and hexamers in solution;[13] hence, it was important to investigate the possible presence of multiple species with similar or different architectures. For this purpose, the data was globally fitted to the bimodal Schulz sphere and Schulz sphere models (ESI†). The calculated SLDs for the hexamer (1.56×10^{-6} Å^{-2}), dimer (1.37×10^{-6} Å^{-2}) and solvent (5.28×10^{-6} Å^{-2}) were held fixed for global fitting. An unphysical volume fraction was obtained for the second spherical species in the bimodal Schulz sphere global fit, clearly indicating that the PgC_3Zn sample has a unimodal distribution. In fact, the data for the PgC_3Zn was fit best to a polydisperse sphere (Schulz sphere) model[21,22] with a chi-sqrt value of 1.156 and a radius of ≈9.4 Å, a result indicating the presence of only one spherical assembly in solution (ESI;† Fig. 1 and 2).

In comparison with the radii of the PgC_3Cu and PgC_3Ni dimers, the radius obtained for the PgC_3Zn dimer is ≈2.4 Å larger, and the size/diameter of the PgC_3Zn dimer (≈18.8 Å) is intermediate between that of a PgC_3Cu/Ni dimer (≈14 Å) and that of a PgC_3Cu/Ni hexamer (≈20 Å). This comparison indicates that PgC_3Cu and PgC_3Ni most likely lose their ligands in solution. As this was the case, we examined the dimensions of the solid-state PgC_3Zn dimer (XRD). The solid-state radius of the PgC_3Zn dimer is ≈9.4 Å and ≈7 Å with and without external pyridine/DMSO ligands, respectively.[16] The geometric dimensions obtained for the PgC_3Zn dimer in the solution phase are nearly identical to those obtained in the solid state. Thus, SANS data analysis for the solvent-solubilized PgC_3Zn dimer not only confirms its spherical shape and structural stability in solution but also reveals the preference for a square pyramidal metal bonding geometry, which differs from the distorted square planar geometry found in other metal-seamed (PgC_3Cu, PgC_3Ni) dimers in solution.

These radii obtained for the PgC_3Zn dimer are also commensurate with those calculated from molecular dynamics simulations of PgC_0Zn dimers with and without 8 ligated molecules. These mixed quantum-classical calculations were performed using the AMBER program suite,[23] with a tight-binding DFT scheme (DFTB3)[24] being used to model the Zn, O, and bridging H atoms as well as the atoms of the ligand. All other atoms of the dimer were treated classically using the gaff2 force field.[25] The simulation results reported here reflect the dynamics of room-temperature gas-phase species. In the absence of the ligands, the average dimer radius was found to be 4.9 ± 0.1 Å, whereas with 8 ligated ammonia molecules the

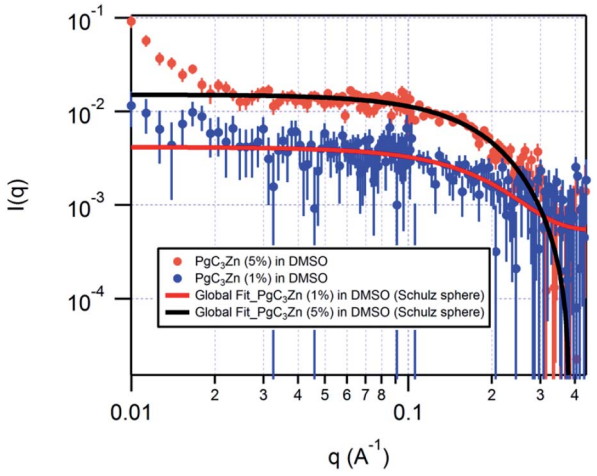

Fig. 2 SANS intensity from the zinc-seamed *C*-propylpyrogallol[4]arene dimer at mass fractions of 1% and 5%. The solid line is the model fit with a polydisperse sphere model. The error bars on the SANS data points represent one standard deviation in the measured intensity. The upturn seen at $q < 0.02$ Å^{-1} is likely due to the presence of a small fraction of aggregates of nanocapsules in solution. Analysis is restricted to larger *q*-values to focus on the scattering from individual nanocapsules.

average radius was 7.1 ± 0.1 Å, with 8 ligated pyridine molecules the average radius was found to be 9.8 ± 0.1 Å, and with 8 ligated DMSO molecules the average radius was found to be 8.4 ± 0.7 Å (the uncertainties here are standard deviations of the average radii as measured from the instantaneous center of mass of the 8 Zn atoms. That is, they reflect the time-dependent thermal fluctuations of the dimer capsule rather than uncertainties in the calculated forces and simulation methodology). The larger uncertainty associated with the calculated average radius for the DMSO-ligated species here derives from the nonlinear bonding at the oxygen and nonplanar bonding at the sulfur in DMSO and the rotation about the oxygen–sulfur bond. In the above ligated species, the calculated radius of the roughly spherical dimer cage itself also differs from that of the non-ligated dimer, being larger by about 0.1 Å in each case.

The solution-phase behavior of PgC_4Zn was further investigated using diffusion-ordered NMR spectroscopy (DOSY). Specifically, we investigated the encapsulation of pyridine within zinc dimers.

Note that we are reporting here the first DOSY NMR study of the metal-seamed pyrogallol[4]arene dimeric framework. The diffusion NMR studies reported by Cohen and co-workers were on hydrogen-bonded pyrogallol[4]arene, octahydroxypyridine[4]arene[26,27] and resorcin[4]arene nanocapsules in $CDCl_3$.[28] Atwood *et al.* have more recently reported DOSY NMR studies on PgC_4Ga hexamers, PgC_4GaZn toroids and hydrogen-bonded $PgC_6\subset$pyrene nanoassemblies in *d*6-acetone.[29]

Capsules of $PgC_4Zn\subset$pyridine for the NMR studies were synthesized by mixing methanolic solutions of *C*-butylpyrogallol[4]arene, zinc nitrate and pyridine in the ratio of 1 : 4 : 14. Sonication yielded a precipitate of zinc dimers. A 2% solution of $PgC_4Zn\subset$pyridine was prepared in *d*6-DMSO for the NMR measurements. Notably, we used a different tail (butyl) here, *versus* the previously studied *C*-propyl tail, as the tail length has been shown to not impact the self-assembled metal-coordinated core architecture of the nanocapsule.

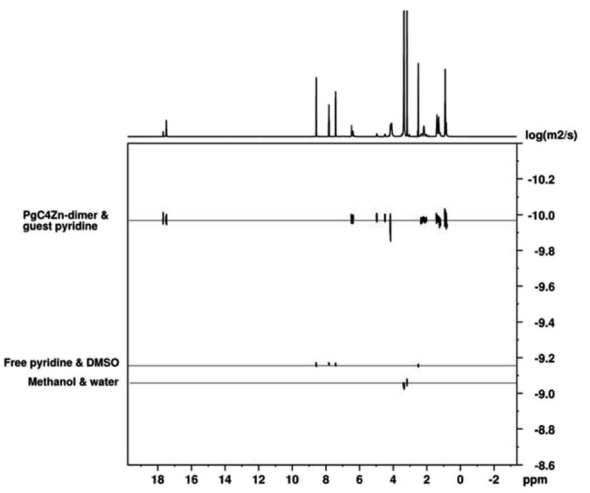

Fig. 3 The DOSY NMR spectra of the [$PgC_4Zn\subset$(pyridine)] dimer. The *Y*-axis on the DOSY plot is displayed as log *D*.

The diffusion coefficients of the phenoxy hydroxyls, alkyl moieties and bound pyridine are similar (Fig. 3), indicating the structural integrity of the PgC_4Zn dimer in DMSO solvent. Overall, the macrocycle/capsule and bound guest pyridine have a diffusion coefficient of 1.04×10^{-10} m^2 s^{-1}. The integration of bound *versus* free pyridine is 1 : 8 suggesting that the external pyridine ligand has exchanged with DMSO. The diffusion coefficients of the "free" pyridine ligand, solvent DMSO, methanol and water are 6.79×10^{-10}, 7.00×10^{-10}, 8.71×10^{-10} and 9.08×10^{-10} m^2 s^{-1}, respectively. The diffusion coefficient of the bound pyridine is about 6.5 times lower than that of a free pyridine.

Overall, the combined neutron scattering, diffusion-ordered NMR spectroscopy and molecular dynamics results indicate (a) the structural stability of the dimer in solution; (b) guest encapsulation; (c) fast external ligand exchange with solvent, which can only be captured through SANS; and (d) an increase in the effective radius of the zinc dimer due to ligation at zinc centers showing a preference for square pyramidal bonding.

The robustness of dimers demonstrated in this study justifies the use of these frameworks for guest encapsulation. Furthermore, the presence of exterior ligands affords valuable insight into the nature of guest-ligand communication. Future studies thus will focus on studying these robust frameworks and on variations in their structural properties in response to varying the encapsulated guest.

Conflicts of interest

There are no conflicts to declare.

Acknowledgements

We thank University of Cincinnati (start-up funds H. K.) and NSF for support of this work (J. L. A.). This work utilized facilities supported in part by the National Science Foundation under Agreement No. DMR-0944772 (S. R. K.) and NSF CHE-89-08304, NIH/NCRR S10 RR022341-01 (cold probe), University of Missouri. Certain trade names and company products are identified to adequately specify the experimental procedure. In no case does such identification imply recommendation or endorsement by the National Institute of Standards and Technology, nor does it imply that the products are necessarily best for the purpose.

Notes and references

1 P. Jin, S. J. Dalgarno and J. L. Atwood, Mixed metal-organic nanocapsules, *Coord. Chem. Rev.*, 2010, **254**, 1760–1768.
2 *Supramolecular Chemistry*, ed. J. W. Steed and J. L. Atwood. John Wiley & Sons, Ltd., 2nd edn, 2009; p. 970.
3 J. Rebek Jr, Simultaneous encapsulation: molecules held at close range, *Angew. Chem., Int.*, 2005, **44**, 2068–2078.
4 F. Durola, H. Dube, D. Ajami and J. Rebek Jr, Control of nanospaces with molecular devices, *Supramol. Chem.*, 2011, **23**, 37–41.

5 S. Di Bella, Second-order nonlinear optical properties of transition metal complexes, *Chem. Soc. Rev.*, 2001, **30**, 355–366.
6 J. L. Atwood, L. J. Barbour, M. J. Hardie and C. L. Raston, Metal sulfonatocalix[4,5]arene complexes: bi-layers, capsules, spheres, tubular arrays and beyond, *Coord. Chem. Rev.*, 2001, **222**, 3–32.
7 S. J. Dalgarno, N. P. Power and J. L. Atwood, Metallo-supramolecular capsules, *Coord. Chem. Rev.*, 2008, **252**, 825–841.
8 H. Kumari, S. R. Kline, N. J. Schuster and J. L. Atwood, Solution structure of copper-seamed C-alkylpyrogallol[4] arene nanocapsules with varying chain lengths, *Chem. Commun.*, 2011, **47**, 12298.
9 H. Kumari, S. R. Kline, N. J. Schuster, C. L. Barnes and J. L. Atwood, Exploring the Ellipsoidal and Core–Shell Geometries of Copper-Seamed C-Alkylpyrogallol[4]arene Nanocapsules in Solution, *J. Am. Chem. Soc.*, 2011, **133**, 18102–18105.
10 A. V. Mossine, H. Kumari, D. A. Fowler, A. K. Maerz, S. R. Kline, C. L. Barnes and J. L. Atwood, Ferrocene as a hydrophobic templating agent with pyrogallol[4]arenes, *Isr. J. Chem.*, 2011, **51**, 840–842.
11 H. Kumari, S. R. Kline, C. L. Dennis, A. V. Mossine, R. L. Paul, C. A. Deakyne and J. L. Atwood, Solution-phase and magnetic approach towards understanding iron gall inks, *Angew. Chemie. Int. Ed.*, 2012, **51**, 9236.
12 H. Kumari, S. R. Kline, W. G. Wycoff, R. L. Paul, A. V. Mossine, C. A. Deakyne and J. L. Atwood, Solution-Phase Structures of Gallium-Containing Pyrogallol[4]arene Scaffolds, *Angew. Chemie. Int. Ed.*, 2012, **51**, 5086–5091.
13 H. Kumari, A. V. Mossine, S. R. Kline, C. L. Dennis, D. A. Fowler, S. J. Teat, C. L. Barnes, C. A. Deakyne and J. L. Atwood, Controlling the Self-Assembly of Metal-Seamed Organic Nanocapsules, *Angew. Chem., Int. Ed.*, 2012, **51**, 1452–1454.
14 A. V. Mossine, H. Kumari, D. A. Fowler, A. Shih, S. R. Kline, C. L. Barnes and J. L. Atwood, Ferrocene species included within a pyrogallol[4]arene tube, *Chem. - Eu. J.*, 2012, **18**, 10258–10260.
15 H. Kumari, S. R. Kline, W. Wycoff and J. L. Atwood, Investigating Structural Alterations in Pyrogallol[4]arene-Pyrene Nanotubular Frameworks, *Small*, 2012, **8**, 3321–3325.
16 N. P. Power, S. J. Dalgarno and J. L. Atwood, Robust and stable pyrogallol[4]arene molecular capsules facilitated via an octanuclear zinc coordination belt, *New J. Chem.*, 2007, **31**, 17–20.
17 A. K. Maerz, H. M. Thomas, N. P. Power, C. A. Deakyne and J. L. Atwood, Dimeric nanocapsule induces conformational change, *Chem. Commun.*, 2010, **46**, 1235–1237.
18 N. Power, S. J. Dalgarno and J. L. Atwood, Guest and ligand behavior in zinc-seamed pyrogallol[4]arene molecular capsules, *Angew. Chem., Int. Ed.*, 2007, **46**, 8601–8604.
19 C. J. Glinka, J. G. Barker, B. Hammouda, S. Krueger, J. J. Moyer and W. J. Orts, The 30 m small-angle neutron scattering instruments at the National Institute of Standards and Technology, *J. Appl. Crystallogr.*, 1998, **31**, 430–445.
20 S. R. Kline, Reduction and analysis of SANS and USANS data using IGOR Pro, *J. Appl. Crystallogr.*, 2006, **39**, 895–900.
21 G. V. Schulz, Highly polymerized compounds. CXXII. The relation between reaction rate and composition of the reaction product in macropolymerization processes, *Z. physik. Chem.*, 1935, **B30**, 379–398.
22 M. Kotlarchyk and S. H. Chen, Analysis of small angle neutron scattering spectra from polydisperse interacting colloids, *J. Chem. Phys.*, 1983, **79**, 2461–2469.
23 D. A. Case, I. Y. Ben-Shalom, S. R. Brozell, D. S. Cerutti, T. E. Cheatham III, V. W. D. Cruzeiro, T. A. Darden, R. E. Duke, D. Ghoreishi, M. K. Gilson, H. Gohlke, A. W. Goetz, D. Greene, R. Harris, N. Homeyer, Y. Huang, S. Izadi, A. Kovalenko, T. Kurtzman, T. S. Lee, S. LeGrand, P. Li, C. Lin, J. Liu, T. Luchko, R. Luo, D. J. Mermelstein, K. M. Merz, Y. Miao, G. Monard, C. Nguyen, H. Nguyen, I. Omelyan, A. Onufriev, F. Pan, R. Qi, D. R. Roe, A. Roitberg, C. Sagui, S. Schott-Verdugo, J. Shen, C. L. Simmerling, J. Smith, R. SalomonFerrer, J. Swails, R. C. Walker, J. Wang, H. Wei, R. M. Wolf, X. Wu, L. Xiao, D. M. York and P. A. Kollman, *AMBER 2018*, University of California, San Francisco, 2018.
24 M. Gaus, Q. Cui and M. Elstner, DFTB3: Extension of the Self-Consistent-Charge Density-Functional Tight-Binding Method (SCC-DFTB), *J. Chem. Theory Comput.*, 2011, **7**, 931–948.
25 J. Wang, R. M. Wolf, J. W. Caldwell, P. A. Kollman and D. A. Case, Development and testing of a general amber force field, *J. Comput. Chem.*, 2004, **25**, 1157–1174.
26 Y. Cohen, T. Evan-Salem and L. Avram, Hydrogen-Bonded Hexameric Capsules of Resorcin[4]arene, Pyrogallol[4]arene and Octahydroxypyridine[4]arene Are Abundant Structures in Organic Solvents: A View from Diffusion NMR, *Supramol. Chem.*, 2008, **20**, 71–79.
27 T. Evan-Salem and Y. Cohen, Octahydroxypyridine[4]arene Self-Assembles Spontaneously To Form Hexameric Capsules and Dimeric Aggregates, *Chem. - Eu. J.*, 2007, **13**, 7659–7663.
28 L. Avram, Y. Cohen and J. Rebek Jr, Recent advances in hydrogen-bonded hexameric encapsulation complexes, *Chem. Commun.*, 2011, **47**, 5368–5375.
29 H. Kumari, S. R. Kline, W. G. Wycoff, R. L. Paul, A. V. Mossine, C. A. Deakyne and J. L. Atwood, Solution-Phase Structures of Gallium-Containing Pyrogallol[4]arene Scaffolds, *Angew. Chemie Int. Ed.*, 2012, **51**, 5086–5091.